Glycation of LDL by Methylglyoxal Increases Arterial Atherogenicity

A Possible Contributor to Increased Risk of Cardiovascular Disease in Diabetes

Naila Rabbani,[1] Lisa Godfrey,[1] Mingzhan Xue,[1] Fozia Shaheen,[1] Michèle Geoffrion,[2] Ross Milne,[2] and Paul J. Thornalley[1]

OBJECTIVE—To study whether modification of LDL by methylglyoxal (MG), a potent arginine-directed glycating agent that is increased in diabetes, is associated with increased atherogenicity.

RESEARCH DESIGN AND METHODS—Human LDL was isolated and modified by MG in vitro to minimal extent (MG_{min}-LDL) as occurs in vivo. Atherogenic characteristics of MG_{min}-LDL were characterized: particle size, proteoglycan-binding, susceptibility to aggregation, LDL and non-LDL receptor–binding, and aortal deposition. The major site of modification of apolipoprotein B100 (apoB100) modification was investigated by mass spectrometric peptide mapping.

RESULTS—MG_{min}-LDL contained 1.6 molar equivalents of MG modification—mostly hydroimidazolone—as found in vivo. MG_{min}-LDL had decreased particle size, increased binding to proteoglycans, and increased aggregation in vitro. Cell culture studies showed that MG_{min}-LDL was bound by the LDL receptor but not by the scavenger receptor and had increased binding affinity for cell surface heparan sulfate–containing proteoglycan. Radiotracer studies in rats showed that MG_{min}-LDL had a similar fractional clearance rate in plasma to unmodified LDL but increased partitioning onto the aortal wall. Mass spectrometry peptide mapping identified arginine-18 as the hotspot site of apoB100 modification in MG_{min}-LDL. A computed structural model predicted that MG modification of apoB100 induces distortion, increasing exposure of the *N*-terminal proteoglycan–binding domain on the surface of LDL. This likely mediates particle remodeling and increases proteoglycan binding.

CONCLUSIONS—MG modification of LDL forms small, dense LDL with increased atherogenicity that provides a new route to atherogenic LDL and may explain the escalation of cardiovascular risk in diabetes and the cardioprotective effect of metformin.
***Diabetes* 60:1973–1980, 2011**

From the [1]Warwick Medical School, Clinical Sciences Research Institute, University of Warwick, University Hospital, Coventry, U.K.; and the [2]Diabetes and Atherosclerosis Laboratory, Ottawa Heart Institute Research Corporation, Ottawa, Ontario, Canada.
Corresponding author: Naila Rabbani, n.rabbani@warwick.ac.uk.
Received 22 January 2011 and accepted 11 April 2011.
DOI: 10.2337/db11-0085
This article contains Supplementary Data online at http://diabetes.diabetesjournals.org/lookup/suppl/doi:10.2337/db11-0085/-/DC1.
© 2011 by the American Diabetes Association. Readers may use this article as long as the work is properly cited, the use is educational and not for profit, and the work is not altered. See http://creativecommons.org/licenses/by-nc-nd/3.0/ for details.

Cardiovascular disease (CVD) is the major cause of premature death in individuals with diabetes and is mainly driven by increased arterial atherosclerosis. Increased risk of atherosclerosis is associated with high levels of LDL and, more particularly, with high levels of small dense LDL (sdLDL) (1). The risk of CVD is increased two- to threefold in diabetes, where the typical increase of sdLDL is two- to threefold (2). Plasma levels of sdLDL correlate with carotid intima-media thickness (3) and are linked to the risk of CVD (4).

The processes associated with the transformation of LDL to sdLDL are not fully understood. Cholesterol ester transfer protein–mediated cholesterol ester/triglyceride exchange between VLDL to LDL with hepatic lipase-mediated hydrolysis is involved, but other metabolic factors, genetic factors, and therapeutic agents influence the processes involved (5,6). Initially, sdLDL was proposed as having increased susceptibility to oxidation ex vivo (7), but surprisingly, some studies of patients with diabetes have not found this (8). Nevertheless, sdLDL has characteristics of increased atherogenicity—increased affinity for arterial proteoglycan (PG) and cell surface non-LDL receptor–binding sites (9,10). Increased atherogenicity of sdLDL may be partly linked to nonoxidative modifications of its major lipoprotein, apolipoprotein (apo) B100.

Metabolic factors linked to increased sdLDL may be evident in diabetes. Methylglyoxal (MG) is a potent dicarbonyl glycating agent formed by the degradation of triosephosphate and metabolized by the glutathione-dependent glyoxalase system (11). The plasma concentration of MG is increased two- to fivefold in patients with diabetes (12), which is likely linked to increased flux of formation of MG in hyperglycemia, associated with diabetes (13) and downregulation of expression of glyoxalase 1 by inflammatory signaling (14). Glycation of LDL by MG is directed to arginine residues in apoB100, forming mainly the hydroimidazolone N_{δ}-(5-hydro-5-methyl-4-imidazolon-2-yl)-ornithine residues (MG-H1), a major advanced glycation end product (AGE) in physiologic systems (15) (Fig. 1*A*). MG-H1 is a major AGE of LDL in healthy people and is increased up to fivefold in the LDL of individuals with type 2 diabetes (16). Diabetic patients receiving treatment with metformin had decreased plasma concentrations of MG (17) and decreased MG-H1–modified LDL (16).

In this report, we describe the effect on atherogenicity of modification of human LDL by MG to physiologic

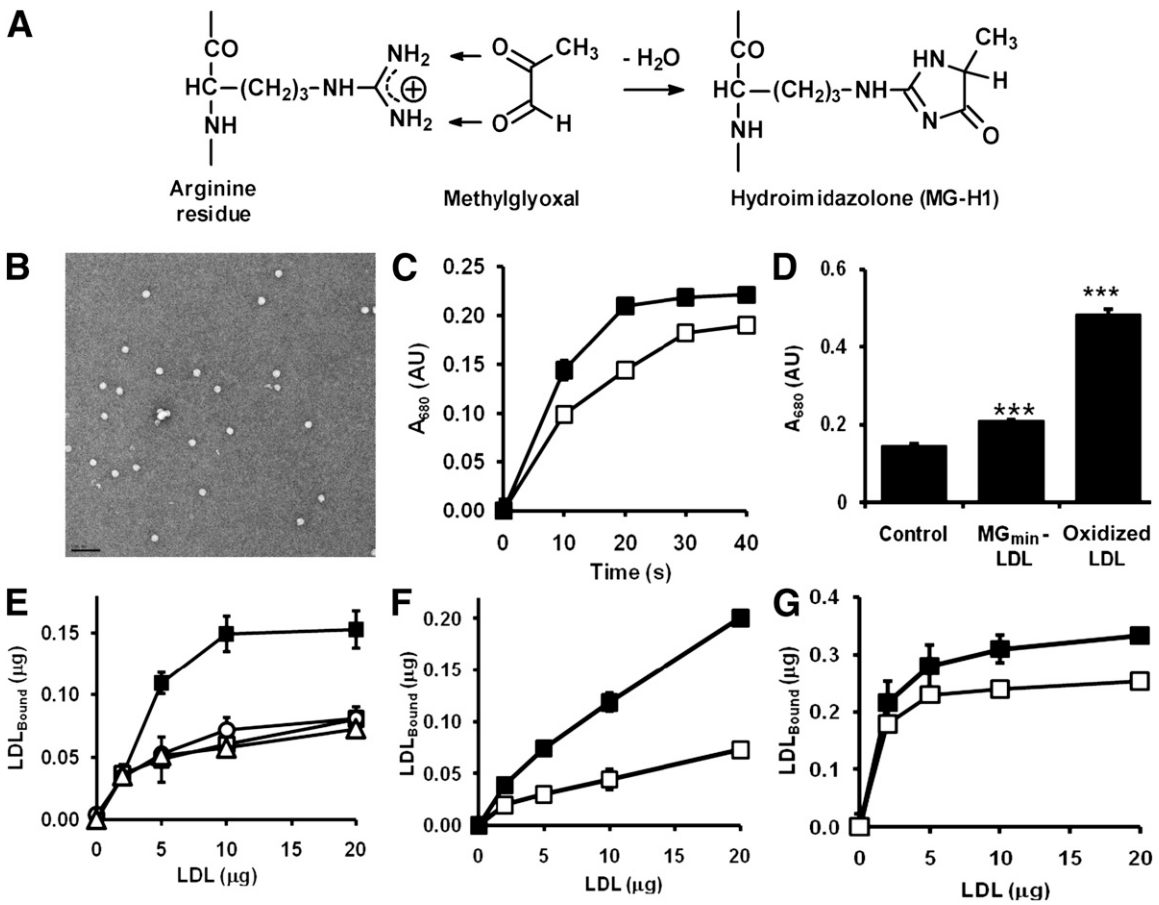

FIG. 1. MG-modified LDL has decreased particle size and increased susceptibility to aggregation and arterial proteoglycan binding. *A*: Reaction of MG with arginine residues form hydroimidazolone MG-H1. *B*: Electron micrograph of MG_{min}-LDL (original magnification ×25,000). *C*: Vortex mixing-stimulated aggregation of LDL: time course—unmodified LDL (-□-□-) and MG_{min}-LDL (-■-■-). *D*: Comparison of aggregation after 20 s for unmodified LDL (Control), MG_{min}-LDL, and oxidized LDL. Proteoglycan binding in cell-free system is shown for biglycan (*E*), aggrecan (*F*), and perlecan (*G*). □, Unmodified LDL; ■, MG_{min}-LDL; ○, MG_{min}-LDL prepared in the presence of aminoguanidine (500 μmol/L); △, glucose-modified LDL, AGE_{min}-LDL. Data are mean ± SD (*n* = 3).

extent. The findings reveal that MG modification is a previously unrecognized route to increased atherogenic sdLDL in diabetes.

RESEARCH DESIGN AND METHODS

LDL and other materials. LDL was isolated from human peripheral venous plasma (16). LDL minimally modified by MG (MG_{min}-LDL) and LDL minimally modified by glucose (AGE_{min}-LDL) were prepared and characterized as described (16). Mildly oxidized LDL was prepared by incubation of LDL (1 mg/mL) with copper sulfate (10 μmol/L) in sodium PBS for 24 h at 37°C, and the content of thiobarbituric acid reactive substances (TBARS) was 3.13 ± 0.88 nmol/mg protein compared with 0.81 ± 0.45 nmol/mg protein in control LDL (16).

Where required, LDL preparations were radiolabeled with ^{125}I using precoated iodination tubes (Fisher Scientific UK Ltd, Loughborough, U.K.), according to the manufacturer's protocol, and purified by gel filtration chromatography. [^{125}I]LDL had specific activity of 337 counts per minute (cpm)/ng protein.

Mouse monoclonal anti-MG-H1 antibody clone 1H7G5 was a gift from Professor Michel Brownlee (Albert Einstein College of Medicine, Bronx, NY). The PGs and glycosaminoglycan used were biglycan and aggrecan from bovine articular cartilage, perlecan from Engelbreth-Holm-Swarm tumor–secreted extracellular matrix (18), and heparin from porcine intestinal mucosa (Sigma-Aldrich, Poole, U.K.; cat nos. B8041, A1960, H4777, and H3149, respectively). Protein concentration of LDL and related derivatives was determined by Bradford and EZQ methods (Invitrogen, Paisley, U.K.).

Electron microscopy. LDL particle size was assessed by electron microscopy. LDL preparations (~150 μg/mL) were applied to grids coated with carbon film containing polystyrene-latex beads of 0.112 μm diameter calibration standard and stained with 2% uranyl acetate (*n* = 3–5 grids for each sample). Samples were examined on a JEOL 2011 transmission electron microscope (200 kV LaB6 cathode; Tokyo, Japan) with a Gatan Ultrascan camera (Pleasanton, CA). The diameter was measured in Gatan Digital Micrograph software using a profile plot.

Cell-free binding of LDL to biglycan, aggrecan, and perlecan and vortex-stimulated aggregation. Binding of LDL to PGs was studied in a cell-free system by incubation of LDL with PG-coated and blocked microplate wells (19). Polystyrene Maxisorp 96-well plates (Nunc, Rochester, NY) were coated with biglycan, aggrecan, or perlecan (50 μg/mL; 100 μL) in PBS overnight at 4°C and blocked with 3% BSA, 1% fat-free milk powder, and 0.05% Tween 20 in PBS for 1 h at 37°C. LDL derivatives in 1% BSA, 140 mmol/L NaCl, 2 mmol/L $CaCl_2$, 2 mmol/L $MgCl_2$, and 20 mmol/L 2-(*N*-morpholino)ethanesulfonate (MES; pH 5.5), were added to the well and incubated for 1 h at 37°C. Unbound LDL was removed, the wells were washed with MES-buffered saline, and bound LDL was determined by the Amplex Red Cholesterol Assay (Invitrogen). LDL aggregation was studied by following aggregation by light scattering at 680 nm induced by vortex mixing of LDL solutions (20,21).

Cell culture studies. Cellular receptor and nonreceptor binding of LDL were studied in cultures of human BJ fibroblasts, hepatocyte-like HepG2 cells, and THP1 macrophages. HepG2 cells and BJ fibroblasts (22) were grown in minimum essential medium (MEM) supplemented with 10% (v/v) FBS, penicillin (100 units/mL), and streptomycin (100 μg/mL) at 37°C in 95% O_2/5% CO_2 and 100% humidity under aseptic conditions in 12-well plates. Cells were washed with Ca^{2+}- and Mg^{2+}-free Hanks' balanced salt solution and incubated with 1.0 mL of MEM containing 20% lipoprotein-deficient serum (LPDS) for 24 h before each experiment.

Surface binding of LDL was determined at 4°C. Cells (8×10^5) were incubated with 5 to 160 μg/mL LDL with 1 μg/mL [^{125}I]LDL tracer in MEM containing 10% LPDS for 3 h. After incubation, cells were washed thrice and

incubated for 1 h with 1.0 mL MEM containing 50 mmol/L NaCl, 10 mmol/L 4-(2-hydroxyethyl)-1-piperazine-ethanesulfonic acid buffer, and 10 mg/mL heparin. The medium was removed and counted for determination of heparin-displaceable LDL. The cells were washed thrice again, dissolved in 0.5 mL of 100 mmol/L NaOH, and counted to determine non–heparin-displaceable LDL.

Where specific binding was determined, LDL binding in the presence of a 10-fold excess of cold LDL was subtracted (23). Some experiments involved preincubation for 2 h with heparinase III (0.2 units/mL) or sodium chlorate (10 mmol/L) for 24 h to remove heparan sulfate and prevent glycosaminoglycan sulfation, respectively. Specific binding was calculated by subtracting the amount of a nonspecific binding, as determined in the presence of a 10-fold excess of unlabeled LDL or MG_{min}-LDL. Competitive inhibition of LDL or MG_{min}-LDL binding was investigated by incubation of [^{125}I]LDL or [^{125}I]MG_{min}-LDL in the presence of 0 to 80 μg/mL of unlabeled MG_{min}-LDL or LDL preparations, respectively.

Plasma clearance and aortal retention of LDL in vivo. Plasma clearance and aortal binding of LDL and MG_{min}-LDL was studied in rats. [^{125}I]LDL or [^{125}I]MG_{min}-LDL (~1 × 10^6 cpm) was injected in the tail vein of 28 male SD rats (body wt ~250 g; Charles River, Margate, U.K.), with and without heparinase III injection 24 h earlier (24). Blood samples (0.20 mL) were taken from the tail vein at 1, 2, 4, 8, 12, 24, 48, and 72 h, and counted for radioactivity. After the last blood sample, rats were killed, and the aorta was removed. This experimentation was performed on U.K. Home Office project license no PPL40/3260.

Analysis of atherosclerotic lesions in aorta of apo E–deficient mice. Aortal localization of MG-modified protein was studied in diabetic atherosclerosis by immunoblotting of aorta of streptozotocin-induced apoE–deficient ($^{-/-}$) mice being fed a high-fat diet (Supplementary Data).

Peptide mapping of MG modification hotspot of apoB100 of LDL. The hotspot of MG modification in apoB100 was located by sequential limited proteolysis with trypsin and Lys-C of delipidated LDL, MG_{min}-LDL, and two-dimensional chromatography with mass spectrometry peptide mapping. LDL (250 μg in 100 mmol/L ammonium bicarbonate [pH 8], 90 μL) was incubated with dithiothreitol (10 mmol/L, 10 L) at room temperature for 1 h. Sodium iodoacetamide (100 mmol/L in water, 10 μL) was added, and samples were incubated at room temperature in the dark for 1 h. The LDL solution was transferred to a glass vial containing butylated hydroxytoluene in methanol (5 μL, 2 mg/mL) and 20% trichloroacetic acid (105 μL), mixed well, left on ice for 10 min, and centrifuged at 10,000*g* for 15 min at 4°C. The supernatant was removed. The pellet was washed with acetone (200 μL) and diethyl ether (200 μL) and dried under argon.

The remaining apoB100 precipitate was suspended in 100 μL of 50 mmol/L ammonium bicarbonate (pH 8) containing 0.1% (w/v) surfactant RapiGest (Waters, Watford, U.K.). Trypsin (1 mg/mL, 6 μL) was added and incubated under argon at 37°C in the dark for 2 h with shaking. The digested sample (suspension of digested LDL) was mixed with 1% formic acid in 10% acetonitrile (1:1, v/v), centrifuged at 10,000*g* for 5 min, and the peptide-containing supernatant was retained.

The tryptic digest (45 μL, 106 μg) was fractionated by gel permeation chromatography (Shodex 2 x KW-800 series, 300 × 8-mm columns in series with a KW-G, 6 × 50-mm guard column; Showa Denko, Tokyo, Japan). The mobile phase was 100 mmol/L $Na_2H_2PO_4$, 140 mmol/L NaCl (pH 7.4), the flow rate was 1 mL/min, and fractions were collected and lyophilized. Peptides were extracted from residual salts by methanol, and solvent was removed under reduced pressure. Half of the recovered peptides were digested exhaustively, and MG-H1 and arginine content were quantified by stable isotopic dilution analysis liquid chromatography-tandem mass spectrometry (LC-MS/MS) (16).

The fraction with the highest MG-H1/arg content was further digested with endopeptidase Lys-C (peptide: protease ratio of 50:1) under argon at 37°C (pH 7.4) in the dark for 2 h. The Lys-C digest was lyophilized, reconstituted in 0.1% trifluoroacetic acid, and desalted (C_{18} ZipTip pipette tips, Millipore, Billerica, MA). Digests were analyzed by nanoflow liquid chromatography-ion trap mass spectrometry with alternating collision-induced dissociation (CID) and electron transfer dissociation (ETD) peptide fragmentation: EASY-nLC interface, flow rate of 300 nL/min, with fluoranthene electron/proton donor-AmaZon mass spectrometer (Bruker Daltonics, Bremen, Germany). CID fragmentation was controlled by SmartFrag (Bruker Daltonics). ETD fragmentation was performed with 500,000 counts of fluoranthene present in the trap for 100 ms and Smart Decomposition set to auto. Spectra were processed using DataAnalysis (Bruker), and the resulting peak lists were subjected to database searching using Mascot (Matrix Sciences, London, U.K.). Good peptide fragmentation was observed, and peptide Mascot scores were >15. Peptides were present throughout the 500-kDa sequence of the protein.

Molecular modeling. R18 of the predicted structure of the *N*-terminal 300 amino acid residue domain of human apoB100, deduced from sequence similarity with vertebrate lipovitellin (25), was modified to an MG-H1 residue. Energy minimization and molecular graphics representation were performed using DS Viewer Pro 5.0 (Accelrys, San Diego, CA).

Statistical analysis. Data are mean ± SD for parametric data and median (upper–lower quartile) for nonparametric data. Significance of difference between mean changes was assessed by Student *t* test and between median changes by Mann-Whitney *U* test.

RESULTS

Minimal modification of LDL by MG decreases particle size and increases tendency toward aggregation and binding affinity for arterial PGs. MG_{min}-LDL had 1.6 molar equivalents of MG modification, 98% of which was MG-H1 (16). Modification of LDL by MG produced a significant decrease in LDL particle size, similar to that of sdLDL (26) (Fig. 1*B*, Table 1). Glycation of LDL by glucose and glycation of LDL by MG in the presence of aminoguanidine, a MG scavenger (27), were without similar effect. MG modification did not change the cholesterol and triglyceride content of LDL.

We next investigated whether MG_{min}-LDL had increased tendency to aggregate and bind PGs. Aggregation of LDL is stimulated experimentally by vortex mixing solutions of LDL. When vortexed for 0 to 40 s, MG_{min}-LDL showed a greater rate and extent of aggregation than unmodified LDL (Fig. 1*C*). Glycation by glucose and glycation by MG in the presence of aminoguanidine produced LDL derivatives that were without similar effect. Oxidized LDL was more susceptible to aggregation than MG_{min}-LDL in this evaluation (Fig. 1*D*). Arginine-directed glycation by MG, however, is a novel nonoxidative modification that stimulates LDL aggregation.

We investigated binding of LDL derivatives to vascular PGs, including the class I small leucine-rich biglycan, the large extracellular PG aggrecan, and the basement membrane PG perlecan; these PGs are all found in regions of atherosclerotic plaque development (28,29). In the cell-free system, MG_{min}-LDL had a higher binding affinity for biglycan than unmodified LDL, glucose-modified LDL, and LDL modified by MG in the presence of aminoguanidine (Fig. 1*E*). MG_{min}-LDL also had increased binding to aggrecan and perlecan than the unmodified control LDL (Fig. 1*F* and *G*).

TABLE 1
Effect of MG modification on the physicochemical characteristics of LDL

	Control LDL		MG_{min}-LDL		
Variable	*n*	Mean ± SD	*n*	Mean ± SD	*P*
LDL size (nm)	70	29.1 ± 1.8	70	26.0 ± 1.7	<0.001
+Aminoguanidine	20	28.4 ± 1.5	20	27.9 ± 1.3	0.33
Cholesterol (mmol/mg protein)	6	2.34 ± 0.07	6	2.29 ± 0.18	0.62
Triglycerides (mmol/mg protein)	4	0.127 ± 0.018	4	0.133 ± 0.027	0.21
TBARS (nmol/mg protein)	4	0.67 ± 0.14	5	0.68 ± 0.12	0.88

LDL minimally modified by MG retains binding to the LDL receptor and increases binding to cell surface heparan sulfate–containing PGs. Binding of LDL to the LDL receptor mediates particle entry into cells (30). We assessed whether MG modification of LDL impaired this process by studying binding of MG_{min}-LDL to human hepatocyte-like HepG2 cells and BJ fibroblasts in vitro. Cell binding of MG_{min}-LDL to HepG2 and BJ cells was not significantly different from that of unmodified LDL (Fig. 2*A* and *B*, respectively). Binding of MG_{min}-LDL was competitive with unmodified LDL, and both had similar affinity constants for specific binding (Supplementary Data). This indicates that MG modification of LDL does not impair uptake of LDL at normal physiologic sites. In the same cells, however, heparin-displaceable binding of MG_{min}-LDL was increased compared with that of unmodified LDL (Fig. 2*C* and *D*). This was blocked when heparan sulfate was removed from the cell surface by prior incubation with heparinase III (Fig. 2*E* and *F*) and when glycosaminoglycan sulfation was suppressed by preincubation of cells with chlorate (Fig. 2*G*). This suggests that MG_{min}-LDL has increased binding to heparan sulfate, non-LDL receptor sites, on the surface of fibroblasts and hepatocytes.

MG_{min}-LDL and LDL had similar binding to human monocyte-derived macrophages, which was not inhibitable by scavenger receptor ligands, suggesting that MG modification does not mediate the recognition of LDL by scavenger receptors (Supplementary Data).

Minimal modification of LDL by MG increases aortal retention in vivo. We assessed if MG_{min}-LDL had increased binding to arterial PGs in vivo. Radiotracer [^{125}I] MG_{min}-LDL or unmodified [^{125}I]LDL was injected into rats and plasma clearance of the lipoproteins determined. Plasma clearance rates were similar for MG_{min}-LDL and unmodified LDL (Fig. 2*H*). On termination of the plasma clearance study, we assessed levels of radiotracer LDL derivative in the aorta. MG_{min}-LDL had significantly increased

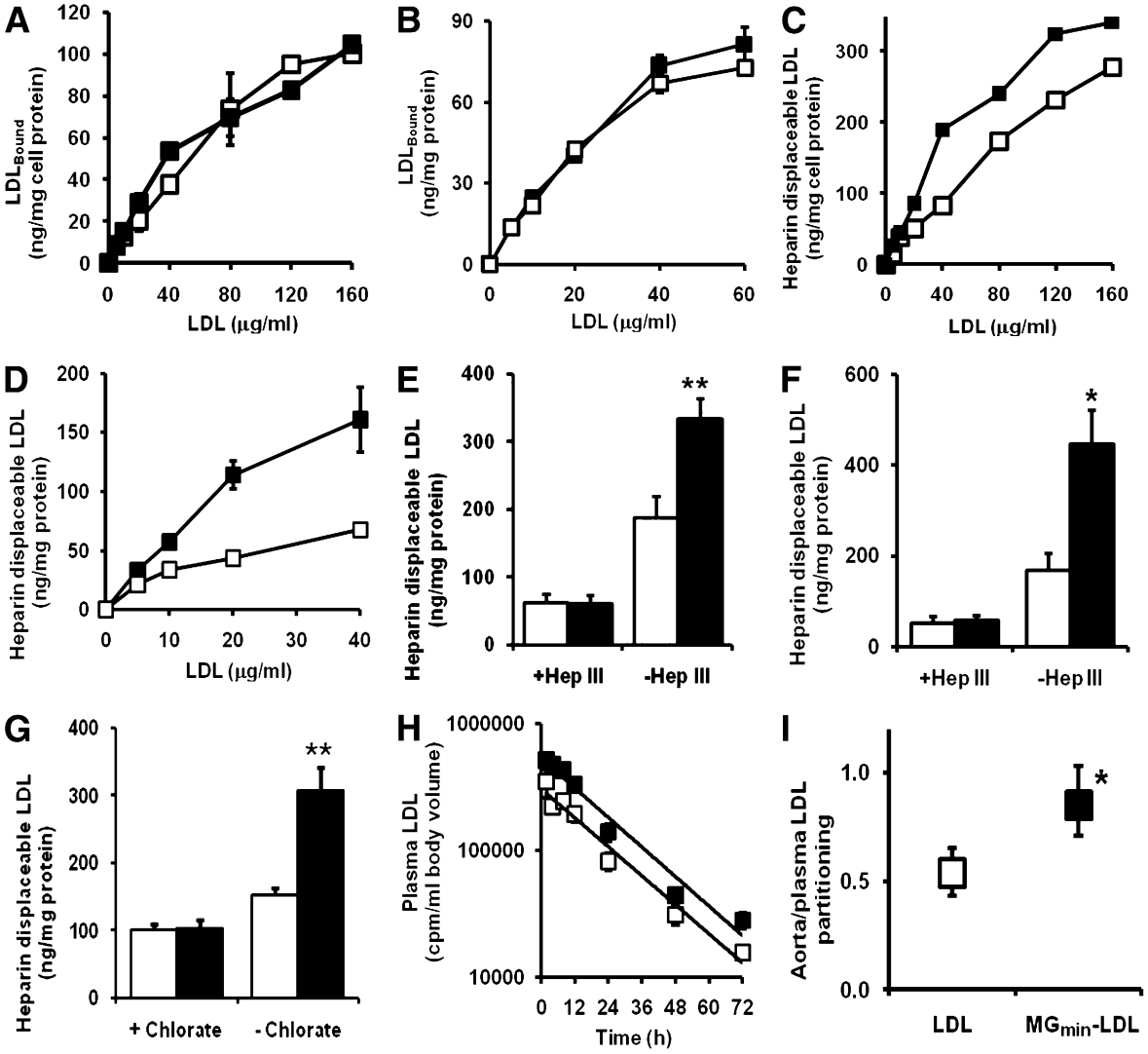

FIG. 2. Preserved LDL receptor binding, increased cellular proteoglycan binding, and aortal retention of MG-modified LDL. Cell binding of LDL and MG_{min}-LDL. Curves for non-heparin–displaceable binding are shown for HepG2 cells (*A*) and BJ cells (*B*). Curves are shown for heparin–displaceable binding for HepG2 cells (*C*) and BJ fibroblasts (*D*). The effect of heparinase III (Hep III) on heparin displaceable binding is shown for HepG2 cells (*E*) and BJ fibroblasts (*F*). *G*: Effect of chlorate inhibition is shown for PG sulfation on heparin-displaceable binding in HepG2 cells. Effect is shown for MG modification on plasma clearance (*H*) and aortal/plasma partitioning (*I*) in vivo. The latter is given as the ratio of radiolabeled LDL: cpm per g wet weight aorta/cpm per mL blood at sacrifice. -□-□- or □ bar, Unmodified LDL; -■-■- or ■ bar, MG_{min}-LDL. Data are mean ± SD (n = 3–6). Plasma LDL radioactivity (cpm) was fit to a single exponential decay curve. *P < 0.05 and **P < 0.01 (t test).

partitioning from blood to the aorta (Fig. 2*I*). This was abolished by prior treatment with heparinase III, suggesting that MG modification of LDL increases retention of LDL in the arterial wall at heparan sulfate–containing PGs.

A well-studied model of diabetic atherogenesis is the high-fat "Western diet" streptozotocin-induced diabetic apo $E^{-/-}$ mouse (30). Serum glucose concentration was ~40 mmol/L, indicative of frank hyperglycemia. Serum LDL was increased 7.5-fold and serum MG concentration 63% (Supplementary Data). We previously found the rate of modification of LDL by MG, $r_{MG\text{-}LDL}$, was directly proportional to concentrations of MG and LDL (16) and hence $r_{MG\text{-}LDL} = k_{MG,LDL}[MG][LDL]$ where [MG] and [LDL] are concentrations of MG and LDL, respectively, and $k_{MG,LDL}$ is the rate constant for the glycation of LDL by MG. The increased concentrations of LDL and MG combine in streptozotocin-induced diabetic apo$E^{-/-}$ mice, therefore, to give a predicted ~12-fold increase of the in situ rate of MG modification of LDL, relative to nondiabetic controls. We examined the location of MG-H1 in sections of aorta of diabetic and control apo$E^{-/-}$ mice by immunohistochemistry. Typical aortal sections showed increased staining for MG-H1 in diabetic mice compared with healthy controls (Fig. 3*A* and *B*).

Site of modification of apoB100 of LDL by MG and predicted impact on structure. The location of MG-H1 residues in apoB100 of MG_{min}-LDL was sought. The presence of MG-H1 residues in apoB100 was confirmed by LC-MS/MS of exhaustive enzymatic digests (16) (Fig. 3*C* and *D*). Glycation of LDL by MG in the presence of heparin did not decrease MG-H1 formation, consistent with the primary site of glycation being located outside of the PG binding site in apoB100 although capable of allosteric interaction with it. We delipidated MG_{min}-LDL and digested the resultant apoB100 with trypsin and fractionated tryptic peptides by gel permeation chromatography. Trypsinization of apoB100 is relatively ineffective (31), albeit improved in the presence of surfactant RapiGest, and large peptides remained (Fig. 3*E*). In replicate subsequent Lys-C digests (n = 4) of MG-H1–rich fractions, MG modification was detected in peptide $DATR_{MG\text{-}H1}FK$ (residues 15–20) of apoB100 extracted from MG_{min}-LDL and not from digests of unmodified LDL (Fig. 3*F*). For identification, this peptide fragmented with CID and all b- and z-ions were detected (Fig. 3*G*). Further supporting evidence was detection of a related MG-H1 peptide $DATR_{MG\text{-}H1}FKHLRK$ $(M+2H)^{2+}$, m/z = 663.54 from MG_{min}-LDL and unmodified dipeptide $(M+2H)^{2+}$, m/z = 636.43, from LDL. This identified R18 a target of MG modification in apoB100 as site B-1a (residues 15–25).

To assess the structural consequences of MG modification of LDL, a molecular graphics prediction of the structure of the MG-modified apoB100 was made. A molecular model was derived from structural similarity of this region of apoB100 to lipovitellin (25) located R18 at the terminal focus of a lattice of seven parallel β-strands. R18 has an intraresidue hydrogen bond (carbonyl O–δNH, bond length 2.29 Å) and a weak ionic interaction with the phenolic OH group of Y27 (bond length 2.94 Å). The PG-binding domain, site B-Ib (84–94), lies at the edge of the seven parallel β-strand lattice held to it by hydrogen bonding of residues L72–K88 and E74–L86 bond lengths 1.78 and 1.87 Å, respectively (Fig. 3*H*). With MG modification, the seven β-strands are all partially distorted and interactions with $R18_{MG\text{-}H1}$ are broken. The PG-binding site B-Ib is raised ~2 Å on the surface as hydrogen bonding interactions with L72 and E74 are lost (Fig. 3*G* and *H*). This provides increased exposure of site B-Ib and likely explains the increased binding affinity of MG_{min}-LDL to PGs.

DISCUSSION

This study identified a novel endogenous modification of LDL, converting it to the proatherogenic form, increasing binding to arterial PGs, and thereby producing increased retention of LDL in the arterial wall.

The decrease in particle size of MG_{min}-LDL with retention of mass of the major components is interpreted as an increase in density, and hence, MG_{min}-LDL is a new type of sdLDL. Measurements of LDL subfraction diameters by electron microscopy established that the mean particle diameter decreases with increasing density (32). Recent studies suggest that the LDL particle has a flattened discoidal shape, with the wide circumference surface a high-density region containing apoB100. Part of apoB100 protrudes into the solvent, producing a lower-density region (33). We speculate that MG modification has the effect of decreasing the protrusion and increasing particle density. A loss of cholesterol esters and a decreased cholesterol/apoB100 ratio is often found in sdLDL in vivo. This is partly linked to the triglyceride/cholesterol ester exchange by the cholesterol ester transfer protein (5). This is not available in the conversion of LDL to $sdMG_{min}$-LDL in vitro, and so the cholesterol/apoB100 ratio remains unchanged.

Modification of LDL by MG was directed to arginine residues of the protein component—mainly apoB100—forming hydroimidazolone MG-H1 residues. This modification is nonoxidative and, hence, does not form oxidized LDL, as judged by the lack of increase in TBARS content; nor was there an increase in methionine sulfoxide, dityrosine, and 3-nitrotyrosine, which are markers of protein oxidation (16). MG may modify basic phospholipids, phosphatidylethanolamine, and phosphatidylserine (34). There appeared to be little modification of nonprotein sites, however, because the estimation of total MG adducts in MG_{min}-LDL by preparation with radiolabeled [^{14}C]MG was similar to the total increase in MG-derived AGEs. By facilitating trapping of LDL by arterial PG, however, MG modification may promote LDL oxidation indirectly (35). LDL was decreased in size by 11% on modification by MG, suggesting that MG modification of LDL causes particle remodelling to an atherogenic form. The sdLDL particles gain entry and are retained in the arterial wall, especially at sites of atherosclerotic plaque lesion development (36).

The initial stages of atherosclerosis in the arterial wall involve the accumulation of aggregates of small lipid droplets and vesicles of up to 400 nm in diameter in the extracellular matrix and the binding of these to PGs (20,21). Characteristic of atherogenic sdLDL, MG-modified LDL had an increased tendency to form aggregates and increased binding affinity for arterial PGs and cell surface heparan sulfate (10). PG binding has been implicated in subendothelial retention of LDL in animal models of atherogenicity (37).

Chemical modification of LDL by arginine-specific modifying agents has been investigated previously. A nonphysiologic arginine-modifying agent, 1,2-cyclohexandione, was used, and LDL with extremely high supraphysiologic extents of modification was prepared: ~66 mol adducts per mol of LDL (44% of total arginine residues). This modified LDL at sites other than the hotspot site discovered in this study and thereby produced a markedly abnormal LDL

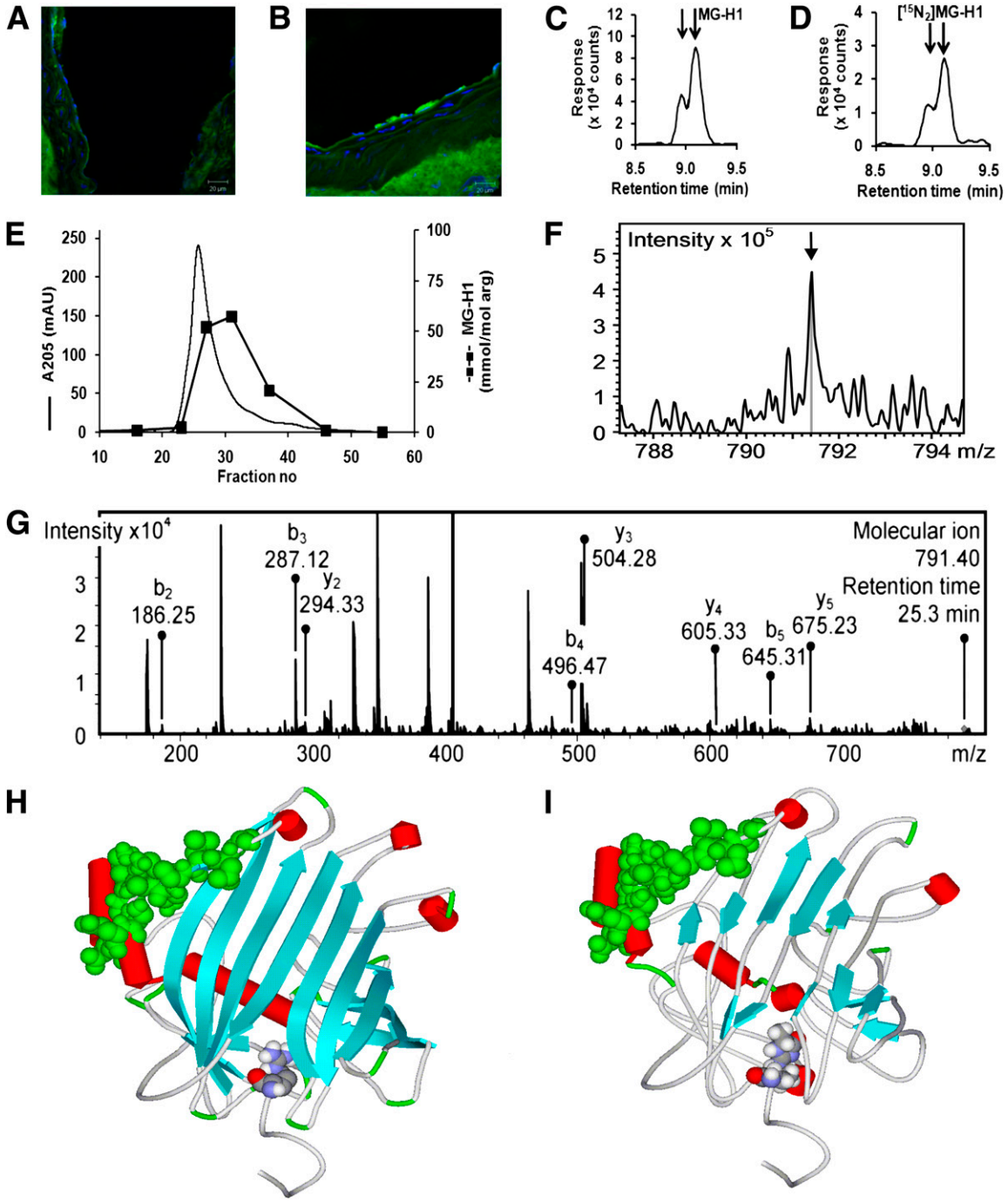

FIG. 3. Aortal accumulation of MG-H1 in diabetic atherosclerosis and proteomic and structural basis of functional change in MG modified LDL. *A* and *B*: Confocal photomicrographs show sectioned aorta in healthy apoE$^{-/-}$ mice immunostained for endogenous MG-H1: healthy control mouse (*A*) and diabetic mouse being fed a high-fat diet (*B*). Immunostaining was visualized with Alexa488 secondary antibody conjugate (green) and nuclei are stained with DAPI (blue). Original magnification ×63; scale bar = 20 μm. Images shown are representative of study group mice (*n* = 7). Proteomic analysis of MG-modified LDL. Detection of MG-H1 in exhaustive enzymatic digests of MG$_{min}$-LDL shows MG-H1 (*C*) and internal standard [^{15}N$_2$]MG-H1 (both showing two partially resolved epimers) (*D*) (15,16). Peptide mapping of apoB100 of MG$_{min}$-LDL shows first dimension chromatography with exhaustive proteolysis locating peptide fractions enriched in MG-H1 (*E*); detection of MG-H1 in peptide DATRFK at R18, m/z = 791.40: molecular ion (*F*) and related CID fragmentation spectrum (*G*). Structural basis of functional change in MG-modified LDL. Molecular models of human apoB100 residues 1–300 are shown for unmodified apoB100 (*H*), and MG-modified apoB100 (*I*). Red cylinders, α-helix; cyan arrows, β-sheets (arrows point to C-terminus); PG binding domain (residues 84–94), green space, fill; and R18 or MG-H1-18, space, fill atom color-coded. (A high-quality digital representation of this figure is available in the online issue.)

with impaired binding to the LDL receptor and PGs (9,38). This masked the effects we found. LDL in vivo has one MG-H1 modification on 2–12% of total LDL (16), and hence, the minimal modification of MG$_{min}$-LDL is appropriate to model MG modification in vivo.

Hotspot modification by MG was located at R18 in apoB100 of LDL. This is the first example of post-translation modification at site B-Ia enhancing LDL binding to PG. Molecular graphics analysis suggested that R18 is a critical stabilizing residue in this domain, and loss of charge after

MG-H1 formation led to loss of β-strand secondary structure, with increased protrusion of the site binding PG on the protein surface. Increased modification of LDL by MG in diabetic apoE$^{-/-}$ mice is also expected because murine apoB48 residues 1–2152 of apoB100, the major protein of LDL in apoE$^{-/-}$ mice (39), has high sequence homology with the same domain of human apoB100 (40), and in situ concentrations of LDL and MG were increased. Although MG modification of LDL is not an oxidative modification, diabetic apoE$^{-/-}$ mice suffer oxidative stress, as indicated by a threefold increase of urinary isoprostanes (41). Increased retention of LDL in the arterial wall by MG modification may synergize with increased oxidative stress to produce increased oxidized LDL in the arterial wall and escalation of atherosclerosis.

MG modification of LDL likely contributes to the increased atherogenicity of LDL in diabetes (16). Agents that scavenge MG, such as metformin, aminoguanidine, and thiazolium compounds, prevented the development of atherosclerosis in diabetic apoE$^{-/-}$ mice (27,42,43). Irbesartan, an angiotensin II receptor blocker, decreased the formation of MG-derived MG-H1 in clinical diabetes (44) and decreased the development of atherosclerotic plaques in diabetic apoE$^{-/-}$ mice (45). Treatment with high-dose thiamine supplements might be expected to prevent diabetic atherosclerosis because this treatment corrected increased MG and dyslipidemia in experimental diabetes (46,47), but this remains to be evaluated. MG is increased in the plasma of patients with diabetes (12) but less in patients treated with metformin (17), with concomitant lowered risk of CVD (48).

Metformin has an antiatherogenic effect that has hitherto been unexplained, but results from this study show it is likely due to a decrease of MG-modified LDL (16). Metformin treatment of patients with type 2 diabetes also decreased sdLDL (49). The nonoxidative nature of the MG modification may partly explain why antioxidant intervention to prevent CVD has been less effective than expected (50). Quantitation of MG-modified LDL may improve epidemiologic CVD risk models, and therapeutics to decrease plasma MG may improve current treatment to decrease CVD in diabetes, renal failure, and in healthy people.

ACKNOWLEDGMENTS

This project was supported by the British Heart Foundation with a personal fellowship to N.R. and a project grant, and also by Heart and Stroke Foundation of Canada grant T6110 to R.M.

No potential conflicts of interest relevant to this article were reported.

N.R. designed the study (except for the apoE$^{-/-}$ mice study), contributed to data interpretation, participated in experimentation, wrote and reviewed the manuscript, and approved the final version. L.G. and M.X. participated in experimentation, contributed to data interpretation, reviewed the manuscript, and approved the final version. F.S. processed and analyzed aortal samples in the apoE$^{-/-}$ study, contributed to data interpretation, reviewed the manuscript, and approved the final version. M.G. performed the apoE$^{-/-}$ mice study, contributed to data interpretation, reviewed the manuscript, and approved the final version. R.M. designed the apoE$^{-/-}$ study, contributed to data interpretation, reviewed the manuscript, and approved the final version. P.J.T. designed the study (except for the apoE $^{-/-}$ mice study), assisted the other authors with experiments, contributed to data interpretation, wrote and reviewed the manuscript, and approved the final version.

Parts of this study were submitted for presentation at the 71st Scientific Sessions of the American Diabetes Association, San Diego, California, 24–28 June 2011.

The authors thank Dr. Julia Smith (Bruker, Coventry, U.K.); Dr. Naomi Yamada-Fowler, Dr. Muhammad Maqsud Anwar, and Tim Orton (Warwick Medical School); and Ian Portman (Imaging Services, Warwick Life Sciences) for technical assistance. The authors thank Professor Jere Segrest (University of Alabama, Birmingham, AL) and Dr. Paul E. Richardson (Coastal Carolina University, Conway, SC) for provision of the Protein Data Bank file of the predicted structure of *N*-terminal 300 amino acid sequence of human apoB100.

REFERENCES

1. Rizzo M, Berneis K, Corrado E, Novo S. The significance of low-density-lipoproteins size in vascular diseases. Int Angiol 2006;25:4–9
2. Tan CE, Chew LS, Chio LF, et al. Cardiovascular risk factors and LDL subfraction profile in type 2 diabetes mellitus subjects with good glycaemic control. Diabetes Res Clin Pract 2001;51:107–114
3. Skoglund-Andersson C, Tang R, Bond MG, de Faire U, Hamsten A, Karpe F. LDL particle size distribution is associated with carotid intima-media thickness in healthy 50-year-old men. Arterioscler Thromb Vasc Biol 1999; 19:2422–2430
4. Rizzo M, Pernice V, Frasheri A, et al. Small, dense low-density lipoproteins (LDL) are predictors of cardio- and cerebro-vascular events in subjects with the metabolic syndrome. Clin Endocrinol (Oxf) 2009;70: 870–875
5. Berneis KK, Krauss RM. Metabolic origins and clinical significance of LDL heterogeneity. J Lipid Res 2002;43:1363–1379
6. Rizzo M, Berneis K, Koulouris S, et al. Should we measure routinely oxidised and atherogenic dense low-density lipoproteins in subjects with type 2 diabetes? Int J Clin Pract 2010;64:1632–1642
7. de Graaf J, Hendriks JC, Demacker PN, Stalenhoef AF. Identification of multiple dense LDL subfractions with enhanced susceptibility to in vitro oxidation among hypertriglyceridemic subjects. Normalization after clofibrate treatment. Arterioscler Thromb 1993;13:712–719
8. Scheffer PG, Bos G, Volwater HG, Dekker JM, Heine RJ, Teerlink T. Associations of LDL size with in vitro oxidizability and plasma levels of in vivo oxidized LDL in type 2 diabetic patients. Diabet Med 2003;20:563–567
9. Anber V, Millar JS, McConnell M, Shepherd J, Packard CJ. Interaction of very-low-density, intermediate-density, and low-density lipoproteins with human arterial wall proteoglycans. Arterioscler Thromb Vasc Biol 1997;17: 2507–2514
10. Galeano NF, Al-Haideri M, Keyserman F, Rumsey SC, Deckelbaum RJ. Small dense low density lipoprotein has increased affinity for LDL receptor-independent cell surface binding sites: a potential mechanism for increased atherogenicity. J Lipid Res 1998;39:1263–1273
11. Thornalley PJ. The glyoxalase system in health and disease. Mol Aspects Med 1993;14:287–371
12. McLellan AC, Thornalley PJ, Benn J, Sonksen PH. Glyoxalase system in clinical diabetes mellitus and correlation with diabetic complications. Clin Sci (Lond) 1994;87:21–29
13. Thornalley PJ. Modification of the glyoxalase system in human red blood cells by glucose in vitro. Biochem J 1988;254:751–755
14. Thornalley PJ. Dietary AGEs and ALEs and risk to human health by their interaction with the receptor for advanced glycation endproducts (RAGE) —an introduction. Mol Nutr Food Res 2007;51:1107–1110
15. Thornalley PJ. Dicarbonyl intermediates in the Maillard reaction. Ann N Y Acad Sci 2005;1043:111–117
16. Rabbani N, Chittari MV, Bodmer CW, Zehnder D, Ceriello A, Thornalley PJ. Increased glycation and oxidative damage to apolipoprotein B100 of LDL cholesterol in patients with type 2 diabetes and effect of metformin. Diabetes 2010;59:1038–1045
17. Beisswenger PJ, Howell SK, Touchette AD, Lal S, Szwergold BS. Metformin reduces systemic methylglyoxal levels in type 2 diabetes. Diabetes 1999;48:198–202
18. Couchman JR, Kapoor R, Sthanam M, Wu RR. Perlecan and basement membrane-chondroitin sulfate proteoglycan (bamacan) are two basement

membrane chondroitin/dermatan sulfate proteoglycans in the Engelbreth-Holm-Swarm tumor matrix. J Biol Chem 1996;271:9595–9602
19. Sneck M, Kovanen PT, Oörni K. Decrease in pH strongly enhances binding of native, proteolyzed, lipolyzed, and oxidized low density lipoprotein particles to human aortic proteoglycans. J Biol Chem 2005;280:37449–37454
20. Oörni K, Pentikäinen MO, Ala-Korpela M, Kovanen PT. Aggregation, fusion, and vesicle formation of modified low density lipoprotein particles: molecular mechanisms and effects on matrix interactions. J Lipid Res 2000;41:1703–1714
21. Pentikäinen MO, Lehtonen EM, Kovanen PT. Aggregation and fusion of modified low density lipoprotein. J Lipid Res 1996;37:2638–2649
22. Goldstein JL, Basu SK, Brown MS. Receptor-mediated endocytosis of low-density lipoprotein in cultured cells. Methods Enzymol 1983;98:241–260
23. Cho BHS, Dokko RC, Chung BH. Oleic, linoleic and linolenic acids enhance receptor-mediated uptake of low density lipoproteins in Hep-G2 cells. J Nutr Biochem 2002;13:330–336
24. Silver PJ, Moreau JP, Denholm E, et al. Heparinase III limits rat arterial smooth muscle cell proliferation in vitro and in vivo. Eur J Pharmacol 1998;351:79–83
25. Flood C, Gustafsson M, Richardson PE, Harvey SC, Segrest JP, Borén J. Identification of the proteoglycan binding site in apolipoprotein B48. J Biol Chem 2002;277:32228–32233
26. Sacks FM, Campos H. Clinical review 163: cardiovascular endocrinology: low-density lipoprotein size and cardiovascular disease: a reappraisal. J Clin Endocrinol Metab 2003;88:4525–4532
27. Thornalley PJ. Use of aminoguanidine (Pimagedine) to prevent the formation of advanced glycation endproducts. Arch Biochem Biophys 2003;419:31–40
28. Evanko SP, Raines EW, Ross R, Gold LI, Wight TN. Proteoglycan distribution in lesions of atherosclerosis depends on lesion severity, structural characteristics, and the proximity of platelet-derived growth factor and transforming growth factor-beta. Am J Pathol 1998;152:533–546
29. Talusan P, Bedri S, Yang S, et al. Analysis of intimal proteoglycans in atherosclerosis-prone and atherosclerosis-resistant human arteries by mass spectrometry. Mol Cell Proteomics 2005;4:1350–1357
30. Goldstein JL, Brown MS. The LDL receptor. Arterioscler Thromb Vasc Biol 2009;29:431–438
31. Yang CY, Kim TW, Weng SA, Lee BR, Yang ML, Gotto AM Jr. Isolation and characterization of sulfhydryl and disulfide peptides of human apolipoprotein B-100. Proc Natl Acad Sci USA 1990;87:5523–5527
32. Shen MMS, Krauss RM, Lindgren FT, Forte TM. Heterogeneity of serum low density lipoproteins in normal human subjects. J Lipid Res 1981;22:236–244
33. Lund-Katz S, Laplaud PM, Phillips MC, Chapman MJ. Apolipoprotein B-100 conformation and particle surface charge in human LDL subspecies: implication for LDL receptor interaction. Biochemistry 1998;37:12867–12874
34. Shoji N, Nakagawa K, Asai A, et al. LC-MS/MS analysis of carboxymethylated and carboxyethylated phosphatidylethanolamines in human erythrocytes and blood plasma. J Lipid Res 2010;51:2445–2453
35. Hurt-Camejo E, Camejo G, Rosengren B, et al. Effect of arterial proteoglycans and glycosaminoglycans on low density lipoprotein oxidation and its uptake by human macrophages and arterial smooth muscle cells. Arterioscler Thromb 1992;12:569–583
36. Björnheden T, Babyi A, Bondjers G, Wiklund O. Accumulation of lipoprotein fractions and subfractions in the arterial wall, determined in an in vitro perfusion system. Atherosclerosis 1996;123:43–56
37. Skålén K, Gustafsson M, Rydberg EK, et al. Subendothelial retention of atherogenic lipoproteins in early atherosclerosis. Nature 2002;417:750–754
38. Mahley RW, Innerarity TL, Pitas RE, Weisgraber KH, Brown JH, Gross E. Inhibition of lipoprotein binding to cell surface receptors of fibroblasts following selective modification of arginyl residues in arginine-rich and B apoproteins. J Biol Chem 1977;252:7279–7287
39. Webb NR, de Beer MC, de Beer FC, van der Westhuyzen DR. ApoB-containing lipoproteins in apoE-deficient mice are not metabolized by the class B scavenger receptor BI. J Lipid Res 2004;45:272–280
40. Segrest JP, Jones MK, Mishra VK, et al. Apolipoprotein B-100: conservation of lipid-associating amphipathic secondary structural motifs in nine species of vertebrates. J Lipid Res 1998;39:85–102
41. Yi X, Maeda N. alpha-Lipoic acid prevents the increase in atherosclerosis induced by diabetes in apolipoprotein E-deficient mice fed high-fat/low-cholesterol diet. Diabetes 2006;55:2238–2244
42. Zhang M, Song P, Guzman MR, Asfa S, Zou MH. Metformin attenuates atherosclerosis in streptozotocin-induced diabetic ApoE-deficient mice through AMP-activated protein kinase. Diabetes 2009;58:A190
43. Forbes JM, Yee LTL, Thallas V, et al. Advanced glycation end product interventions reduce diabetes-accelerated atherosclerosis. Diabetes 2004;53:1813–1823
44. Rabbani N, Adaikalakoteswari A, Rossing K, et al. Effect of Irbesartan treatment on plasma and urinary markers of protein damage in patients with type 2 diabetes and microalbuminuria. Amino Acids. 8 March 2011 [Epub ahead of print]
45. Candido R, Allen TJ, Lassila M, et al. Irbesartan but not amlodipine suppresses diabetes-associated atherosclerosis. Circulation 2004;109:1536–1542
46. Babaei-Jadidi R, Karachalias N, Ahmed N, Battah S, Thornalley PJ. Prevention of incipient diabetic nephropathy by high-dose thiamine and benfotiamine. Diabetes 2003;52:2110–2120
47. Babaei-Jadidi R, Karachalias N, Kupich C, Ahmed N, Thornalley PJ. High-dose thiamine therapy counters dyslipidaemia in streptozotocin-induced diabetic rats. Diabetologia 2004;47:2235–2246
48. Bailey CJ. Metformin: effects on micro and macrovascular complications in type 2 diabetes. Cardiovasc Drugs Ther 2008;22:215–224
49. Ohira M, Miyashita Y, Ebisuno M, et al. Effect of metformin on serum lipoprotein lipase mass levels and LDL particle size in type 2 diabetes mellitus patients. Diabetes Res Clin Pract 2007;78:34–41
50. Kris-Etherton PM, Lichtenstein AH, Howard BV, Steinberg D, Witztum JL; Nutrition Committee of the American Heart Association Council on Nutrition, Physical Activity, and Metabolism. Antioxidant vitamin supplements and cardiovascular disease. Circulation 2004;110:637–641